Journal of Renewable Materials

Tech Science Press

DOI: 10.32604/jrm.2022.021528

ARTICLE

Characterization of Potential Cellulose from *Hylocereus Polyrhizus* (Dragon Fruit) peel: A Study on Physicochemical and Thermal Properties

Nurul Hanan Taharuddin[1], Ridhwan Jumaidin[2,*], Muhd Ridzuan Mansor[1], Fahmi Asyadi Md Yusof[3] and Roziela Hanim Alamjuri[4,*]

[1]Fakulti Kejuruteraan Mekanikal, Universiti Teknikal Malaysia Melaka, Hang Tuah Jaya, Melaka, Malaysia

[2]Fakulti Teknologi Kejuruteraan Mekanikal dan Pembuatan, Universiti Teknikal Malaysia Melaka, Hang Tuah Jaya, Melaka, Malaysia

[3]UNIKL MICET, Taboh Naning, Alor Gajah, Melaka, Malaysia

[4]Faculty of Tropical Forestry, Universiti Malaysia Sabah, Jalan UMS, Sabah, Malaysia

[*]Corresponding Authors: Ridhwan Jumaidin. Email: ridhwan@utem.edu.my; Roziela Hanim Alamjuri. Email: rhanim@ums.edu.my

Received: 19 January 2022 Accepted: 30 March 2022

ABSTRACT

The strict environmental regulations to overcome the drawbacks of consumption and disposal of non-renewable synthetic materials have motivated this investigation. The physical, chemical, morphological, and thermal properties of *Hylocereus Polyrhizus* peel (HPP) powder obtained from the raw materials were examined in this study. The physical properties analyzes of *Hylocereus Polyrhizus* peel (HPP) powder discovered that the moisture content, density, and water holding capacity were 9.70%, 0.45 g/cm^3, and 98.60%, respectively. Meanwhile, the chemical composition analysis of *Hylocereus Polyrhizus* peel (HPP) powder revealed that the powder was significantly high in cellulose contents (34.35%) from other bio-peel wastes. The crystallinity index of *Hylocereus Polyrhizus* peel (HPP) powder was 32.76%, according to further X-ray diffraction (XRD) analysis. The thermal stability of *Hylocereus Polyrhizus* peel (HPP) powder was examined using thermogravimetric analysis (TGA) and found thermally stable at 204°C. The morphological study via scanning electron microscopy (SEM) showed a shriveled and irregular geometry surface. *Hylocereus Polyrhizus* peel (HPP) powder demonstrated the peak in the range representing the major functional groups responsible for pectin's properties. Thus, the findings revealed that the *Hylocereus Polyrhizus* peel (HPP) powder has the potential for the development of biodegradable and renewable materials.

KEYWORDS

Hylocereus Polyrhizus; dragon fruit; peel; natural fiber; biodegradable materials

Nomenclature

θ	Theta

1 Introduction

There are billions of synthetic materials that end up in landfills and on beaches every year. The usage of petroleum-derived synthetic materials endangers the environment since these products release greenhouse

gases throughout their life cycle. Zero waste consciousness and people's awareness worldwide resulted in an increasing trend toward efficient utilization of natural resources. Over the last few decades, there has been a surge in interest in bio-based materials, such as biofibers, biopolymers, and biocomposite materials, which play an important part in replacing synthetic materials [1,2]. Biocomposites are redefining material engineering research because of their numerous advantages, including renewability, lightweight, minimized energy consumption, usability, and environmental friendliness [3]. The use of lignocellulosic fibers as reinforcement has many benefits and drawbacks. Many published studies have shown that lignocellulosic fibers' compatibility with other biopolymers has improved throughout time [4]. The hydrophilicity and wide crosslinking of lignocellulosic fibers have limited this compatibility, resulting in poor interfacial adhesion and mechanical properties on both sides of the interface. Moisture has a significant impact on the dimensional stability of these bioplastics. As a result, surface treatments are widely used for polymeric matrixes so that the effectiveness of lignocellulosic fibers and natural reinforcement adhesion can be achieved [5].

Natural fibers have been used as a traditional source of cellulosic fibers in many places. Cotton, flax, jute, sisal, curaua, hemp, and agricultural by-products such corn, wheat, rice, sugarcane, pineapple, banana, and coconut are among the most important contributions [6]. A fiber's structure is determined by the size and placement of unit cells in it, which also influences its characteristics and the properties of the polymeric composite fiber. According to Jamal Tarique et al. [7], the amount of each element, as well as the form and quality of the fibers are dependent upon the plant species, crop production, extraction site, plant age, plant section harvested, and soil conditions under which they were farmed. Amongst the most significant obstacles to the large-scale production of lignocellulosic-based composites is the inability to manage certain parameters.

Hylocereus Polyrhizus (dragon fruit), also known as "buah naga" in Malay, has carved out a large niche in the exotic and domestic fruit markets. Dragon fruits were initially introduced in Malaysia in 1999 in the states of Setiawan, Johor, Kuala Pilah, and Negeri Sembilan [8], whereas annual production is estimated to be about 10,961 tons [9]. The *Hylocereus Polyrhizus* is consumed as fresh fruit, with the skin peeled away. They are also refined into juice, jams, syrups, and other commercial products, as shown in Table 1. The peel, which is considered waste from the processing of *Hylocereus Polyrhizus*, represents around 22% of fruit [10].

Table 1: *Hylocereus Polyrhizus* peel in various commercial applications

No.	Potential applications	References
1.	Bioplastic from peel pectin	[11]
2.	Natural dye in food	[12]
3.	Raw material for lipsticks	[13]
4.	Renewable adsorbents for water purification	[14]
5.	Poultry diet for laying hens	[15]

The present tendency in fresh fruit consumption has resulted in a massive volume of peel as waste. Up to now, several studies have explored the utilization of dragon fruit peel waste. One study by Lee et al. [16] examined the reuse of discarded dragon fruit peels as natural reductants as an alternative to conventional hazardous reductants for graphene-based material synthesis. In another study, dragon fruit peel extract was synthesized into silver nanoparticles and used as an antiseptic mouthwash [17]. Prastiya et al. [18] found that the addition of various concentrations of peels of dragon fruit in rabbit feed bio supplement has good implications for several aspects of rabbit performance.

Work has been done by a previous study on the physicochemical composition of *Hylocereus Polyrhizus* peel [11,19]. However, there has been little experimental evidence in the literature related to the preparation

and characterization of biocomposite using *Hylocereus Polyrhizus* peel as reinforcement as well as the investigation related to the thermal properties of the peel.

This study, therefore, was set out to investigate the physical, chemical, morphological, and thermal properties of the *Hylocereus Polyrhizus* peel by particle size distribution, density, moisture content (MC), water holding capacity (WHC), chemical composition investigation, scanning electron microscopy (SEM), Fourier transform infrared (FTIR), X-ray diffraction (XRD), and thermogravimetric analysis (TGA). This acquires more knowledge about the possibility of extracting value-added compounds from the *Hylocereus Polyrhizus* peel for a variety of applications.

2 Materials and Methods

Hylocereus Polyrhizus was purchased in a local market in Bangi, Selangor. The *Hylocereus Polyrhizus* peels (HPP) were separated from the flesh first and then cleaned with running water to remove dirt and unwanted particles. Afterward, the peels were chopped into small dice (2–3 cm^2) using a stainless-steel cutter. The peels were dried for two days until they reached a consistent weight. The dried peels were then grounded using a disk mill machine FFC-15 model (Tianhong, Hebei, China) to powder form and kept in a desiccator to prevent further moisture uptake. Upon analysis, HPP powder was heated in an air circulating oven at 105°C for 24 h or until a constant weight was achieved to remove unpredictable moisture absorption. Fig. 1 shows the overall process in the preparation of HPP powder.

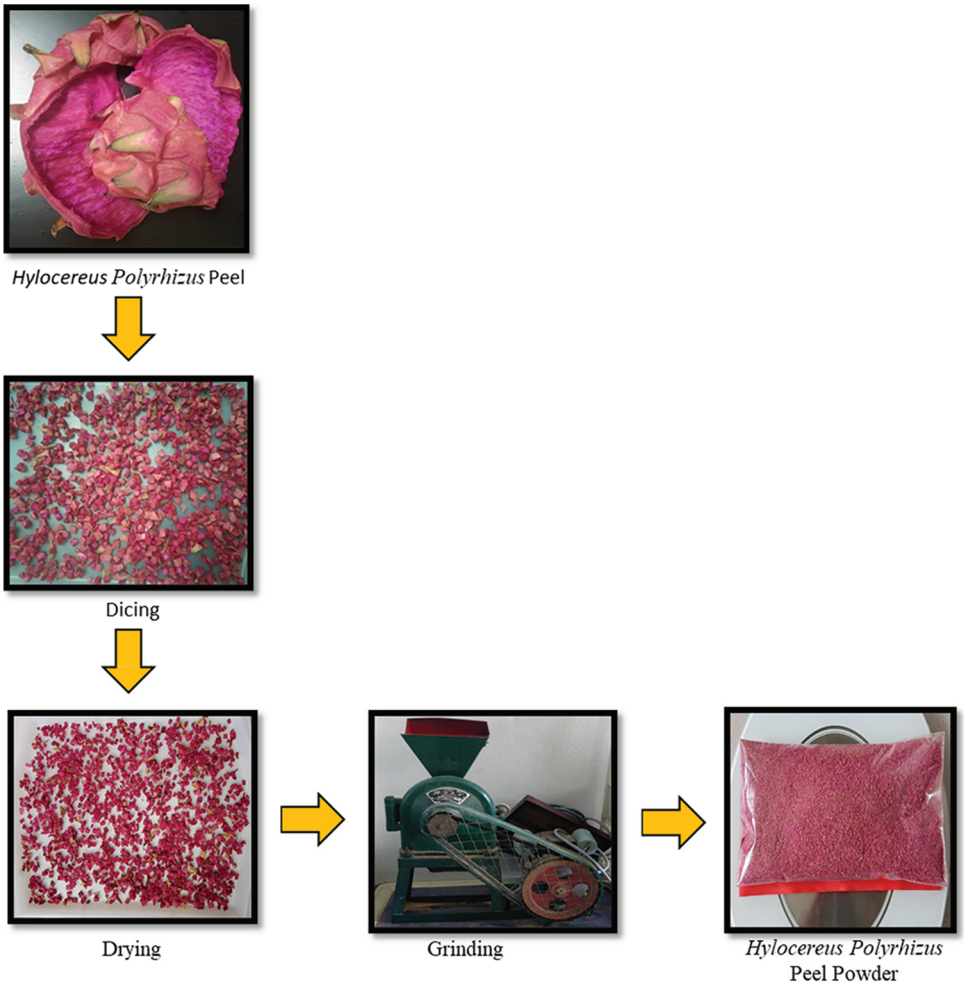

Figure 1: Preparation of *Hylocereus Polyrhizus* peel powder

2.1 Physical Properties

2.1.1 Particle Size

A Mastersizer 3000 (Malvern Instruments Ltd., United Kingdom) equipped with dry dispersion units (Aero S) was used to measure the particle size. In a constant stream of air, the dry sample of *Hylocereus Polyrhizus* peel powder was distributed and uniformly delivered to the measuring cell. The device consists of a laser light source, light processing optics, a cell, a lens, and a multi-element detector. The multi-element detector provides the diffraction pattern. Data processing was needed for the deconvolution of the diffraction data, as well as for volumetric particle size distribution, related data processing, and reporting. The optical unit is the center of the system, designed to transmit red laser light and blue light through the sample. The light was transmitted to a detector, which generated data from light scattering caused by particles in the sample—the measuring cell functions as an interface between the dispersion unit and the optical unit [20,21].

Dry dispersion units were used to distribute the dry sample through the measuring cell with a measuring range of 0.1–3500 μm. The peel powder weighed approximately 2.5 g was placed into the hopper on the vibrating tray before being transported in the direction of the venturi nozzle to the measuring cell. The blue light (λ = 470 nm) was used to capture the background, while the red light (λ = 632.8 nm) was used to detect particles. The rotation speed was 2750 rpm, and the Mie scattering model was applied, with a particle refraction index of 1.468 and particle absorption index of 0.01.

2.1.2 Density

An AccuPyc II 1340 pycnometer gas (Micromeritics Instrument Corp., Norcross, GA, USA) analyzer with the flow of helium gas was used to determine the density of the samples. The samples were oven-dried for 24 h at 105°C to eliminate the moisture content inside the peels. Before placing in the pycnometer, the samples were dried and kept in a desiccator to remove any lingering water traces. Based on measurements made at a temperature of 27°C, Eq. (1) was used to calculate the densities of the samples. The average value was calculated after accumulating five measurements.

$$\rho = \frac{m}{V} \tag{1}$$

where, m = mass (g), V = volume (cm^3).

2.1.3 Moisture Content (MC)

Five samples were examined for moisture content. The samples were heated for 24 h in a 105°C air circulated oven. The moisture content of the samples was determined by weighing them before, W_i, and after, W_f, heating as stated in Eq. (2).

$$\text{Moisture content } (\%) = \left(\frac{W_i - W_f}{W_i}\right) \times 100 \tag{2}$$

2.1.4 Water-Holding Capacity (WHC)

The amount of water that 1 g of dried material can hold expresses a substance's water-holding capability. The experiment was conducted using a HERMLE Z306 universal centrifuge (Hermle Labortechnik GmbH, Germany) using a technique devised by Ibrahim et al. [22]. A powder sample (3 g) was submerged in 25 ml of distilled water in a pre-weighed centrifugal tube ($M_{initial}$). After centrifuging at 3000 rpm for 25 min, the supernatant was removed, and the remaining residue was dried in an air circulation oven at 50°C for 30 min before being weighed again (M_{final}). The test was performed three times until the mass of the tested powder sample was consistent. As a consequence, as stated in Eq. (3), the WHC % was estimated by averaging three readings.

$$\text{Water Holding Capacity } (\%) = \left(\frac{M_{final} - M_{initial}}{M_{initial}}\right) \times 100 \quad (3)$$

2.2 Chemical Composition

The ash, crude fiber, and carbohydrate content of HPP powder were determined during the experiment. Adapted from Hazrati et al. [2], the methodologies used to explore acid detergent fiber (ADF), neutral detergent fiber (NDF), ash, crude fiber, lignin, hemicellulose, and cellulose in HPP powder were used. The chemical composition of HPP powder was determined using the ADF and NDF. Eqs. (4) and (5) were used to calculate the amounts of hemicellulose and cellulose.

$$\text{Cellulose} = \text{ADF} - \text{lignin} \quad (4)$$

$$\text{Hemicellulose} = \text{NDF} - \text{ADF} \quad (5)$$

2.3 Scanning Electron Microscope (SEM)

The samples' surface morphology was determined using the Hitachi S-3400N scanning electron microscope (Hitachi Science Systems Ltd., Japan). To establish an electron beam, the samples were coated with a layer of gold, and a 20 kV voltage was delivered through them in a high vacuum environment. The electrons were coupled to the sample atoms and generated signals that provided a report on the surface topography by generating high-resolution images.

2.4 Fourier Transform Infrared (FTIR) Analysis

The chemical composition and structure of the sample were determined using Fourier transform infrared (FTIR) Spectroscopy. Spectra of the sample were obtained using JASCO FTIR-6100 Spectrometer (JASCO Corporation, Japan). Spectrum was plotted between 4000–400 cm^{-1} wavenumbers.

2.5 X-ray Diffraction (XRD) Analysis

A 2500 X-ray diffractometer (Instrument-Rigaku, Tokyo, Japan) with an angular range of 5 to 60° (2θ) and a scattering speed of 0.02θ s^{-1} was used for the XRD analysis. 35 mA and 40 kV were chosen as the operating current and voltage, respectively. Using the approach of Segal et al. [23], the crystallinity index (CI) of the sample was quantitatively determined from the diffraction intensity data. Eq. (6) was used to get the crystallinity index (%).

$$\text{Crystallinity Index } (\text{CI}) = \frac{I_{002} - I_{am}}{I_{002}} \times 100\% \quad (6)$$

where I_{002} is the diffraction intensity close to 2θ = 22° and represents a crystalline material; I_{am} is the diffraction intensity close to 2θ = 18° and refers to amorphous material in cellulosic fibers.

2.6 Thermogravimetric Analysis (TGA)

Thermogravimetric analysis was employed to characterize the material's thermal degradation behavior in terms of weight loss owing to temperature increase. TGA/DSC 3+ (Mettler-Toledo AG, Analytical, Switzerland) was used in the testing. The weight samples range was 10 ± 2 mg. In an aluminum pan, the test was conducted at a temperature range of 25°C to 600°C at a heating rate of 10 °C min^{-1} in a dynamic nitrogen environment.

3 Results and Discussion

3.1 Physical Properties of Hylocereus Polyrhizus Peel

3.1.1 Particle Size Distribution

The effective stress transmitted between the reinforcement and the matrix has a significant impact on composite material strength. The key parameters that impact the mechanical characteristics of the material are particle/matrix interfacial strength, particle size distribution, and particle loading [24]. The particle size distribution of HPP powder is as shown in Fig. 2. According to the graph, the minimal distribution represents 10% of the particles, and the greatest distribution accounted for 90% of the particles fell within the dimensions of fewer than 189 μm and less than 1310 μm, respectively. The HPP had a diameter of less than 590 μm on average. The smaller the diameter of the fiber, the stronger it is, yet the cost grows as the diameter lowers [25].

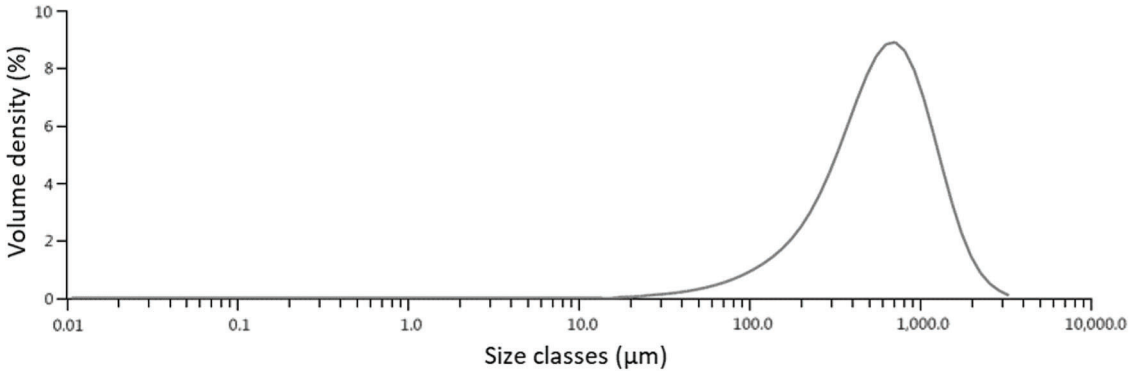

Figure 2: Particle size distribution of *Hylocereus Polyrhizus* peel powder

3.1.2 Density and Moisture Content

By taking an average of five duplicates of each specimen, the density of each specimen was calculated. Table 2 shows the density and moisture content of HPP powder. The density value reported in this work was in agreement with the range of various natural fiber densities reported in other published studies of 0.45 g/cm^3 [26,27]. Biomaterials' low density made them more appealing for biocomposite manufacturing than artificial composite materials such as fiberglass [28]. Furthermore, the moisture content of the HPP powder in this study was approximately 9.70% (dry basis). This value was in good agreement with the reported work by previous studies on HPP powder, in which the values were in the range of 3.30%–10.66% [29–31]. This could be because the fiber's biological qualities were reflected. Apart from that, it might be a useful sign to take into account the material selection process when using fiber as a composite reinforcement [32]. However, the moisture content investigation revealed that the HPP powder had a low moisture content of 9.70%, respectively, compared to cassava [26], corn stalk [22], and arrowroot fiber [7]. This could be owing to the presence of the hydroxyl group in HPP powder's cellulose and lignin.

Table 2: Physical properties of *Hylocereus Polyrhizus* peel powder

Content	*Hylocereus polyrhizus* peel
Moisture content (%)	9.70
Density (g/cm^3)	0.45
Water holding capacity (%)	98.60

3.1.3 Water Holding Capacity

The ability of a material to retain water is a necessary need for the manufacture of composite materials. Some of the reasons were due to their significant influence in terms of dimensional stability, porosity, tensile strength, and swelling behavior of natural composite materials [22]. Based on the value of HPP powder that has a hygroscopic nature, it held the highest amount of water (98.6%) compared to the other fiber samples such as cassava [33], cornhusk [22], and arrowroot [7], all of which possessed a high hydrophilic feature. This remark pertained to the low cellulose component of the HPP powder's composition. Cellulose prevented water from penetrating the intermolecular fiber chain by reducing free volume [34].

3.2 Chemical Composition

The presence of cellulose, lignin, and hemicellulose in HPP powder is one of the most relevant findings in the study of fiber composition. According to Table 3, the chemical composition analysis results were compared to those of prior studies. It was discovered that the cellulose content of HPP powder (34.45%) was significantly higher than the cellulose content of passion fruit peel fiber (28.58%) and prickly pear fruit peel (27.00%). Furthermore, the cellulose percentage of HPP powder was higher than that of cellulose derived from other bio-peel waste, such as cucumber peels, banana peels, orange peels, and mango peels, which were 18.22%, 16.9%, 11.93%, and 9.19%, respectively [35,36]. Additionally, the hemicellulose content of HPP fiber was not detected. These findings were consistent with the results of Bakar et al. [19] and Chia et al. [29], who conducted the same study of fiber. Furthermore, the lignin content of HPP powder (6.73%) was significantly lower than the other peel of fiber, such as passion fruit peel (36.18%). This could be since the percentage of amorphic (lignin, hemicellulose) and crystalline (cellulose) components in natural fibers vary depending on the location and condition of the plant [9]. Chen et al. [37] explained that cellulose is a critical component of natural fiber structure and plant structural strength. The amount of lignin present in the fibrous residue, on the other hand, was evaluated to assess the relative number of resistant components present in the fibrous residue, which plays an important role in the strength and stiffness of the fiber-based walls [2].

On the other hand, natural fibers mainly comprise holocellulose (hemicellulose, cellulose), lignin, crude fiber, and ash. Increased composite tensile strengths were achieved by introducing high cellulose amounts, which allowed for better matrix interactions [38]. When natural fibers were mixed with thermoplastic starch and its derivatives, the mechanical properties of the composite were significantly improved [39]. The chemical similarity between matrix and fibers was discovered to contribute to this property, resulting in optimal composite compatibility [40]. Numerous researches have established the optimal performance of polymer-based biodegradable composites [41]. According to Uitterhaegen et al. [42], inconsistency in fibers could attribute to differences in lignin content or origin, as well as differences in bioplastic manufacturing techniques.

Table 3: Comparative chemical composition of *Hylocereus Polyrhizus* peel powder with other cellulose fibers

Material	Cellulose (%)	Hemicellulose (%)	Lignin (%)	Ash (%)	Crude fiber (%)	Ref.
Hylocereus Polyrhizus peel	34.45	ND	6.73	17.40	27.63	Current study
Hylocereus Polyrhizus peel	9.25	–	37.18	–	–	[19]
Hylocereus Polyrhizus peel	–	–	–	14.29	31.40	[29]
Prickly pear fruit peel	27.00	–	2.40	11.50	–	[43]
Sugarcane peel	7.15	27.52	47.73	–	–	[44]

(Continued)

Table 3 (continued)

Material	Cellulose (%)	Hemicellulose (%)	Lignin (%)	Ash (%)	Crude fiber (%)	Ref.
Passion fruit peel	28.58	23.01	36.18	5.71	–	[45]
Dioscorea Hispida tubers	5.63	4.36	2.79	1.28	–	[2]
Arenga Pinnata (Sugar Palm)	43.88	7.24	33.24	1.01	–	[46]
Cymbopogan citratus leaves	37.56	29.29	11.14	4.28	–	[47]
Pandanus amaryllifolius leaves	48.79	19.95	18.64	1.08	–	[40]
Limonia Acidissima (wood apple) shell	41.28	27.01	28.31	–	–	[48]

Note: ND = Not detected.

3.3 Scanning Electron Microscope (SEM)

The microstructures of the HPP powder are shown in Figs. 3a and 3b, respectively. The peeled surface appeared shriveled and had irregular geometry. The finding was in agreement with studies conducted by Chia et al. [29] and Bakar et al. [19] for the drum drying and spray-drying of dragon fruit peel powder. The shriveled look might be related to the sluggish drying rate during the manufacture of the peel powder, as Tonon et al. [49] found that when the inlet air temperature was low, most powder particles stay shrunk with a shriveled surface. Meanwhile, Alamilla-Beltrán et al. [50] stated that the physical features of the crust, which might be flexible and collapsed (when low and intermediate temperatures were used) or stiff and porous (when high temperatures were employed), could explain morphological variations between powders formed at various temperatures. Similarly, Gan et al. [51] found that due to the physical grinding process performed on a millstone, the powders particle were subjected to friction and shearing force randomly, resulting in the powder surfaces being rough and irregular.

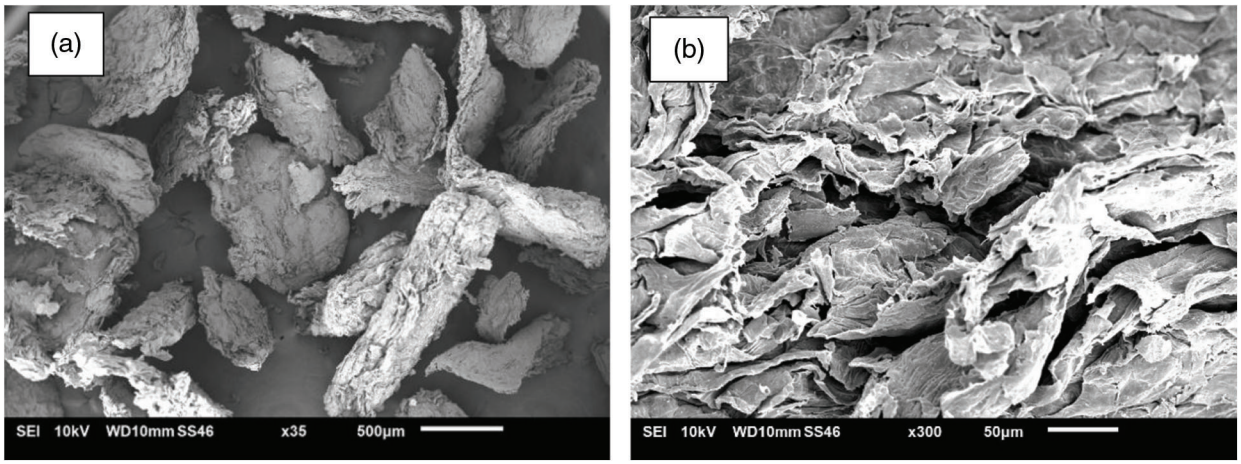

Figure 3: SEM of *Hylocereus Polyrhizus* peel powder surface structure (a) 35X magnification (b) 300X magnifications

3.4 Fourier Transform Infrared (FTIR) Analysis

The FTIR technique was used to investigate the functional groups available in *Hylocereus Polyrhizus* peel powder. In the region between 4000–400 cm^{-1} of FTIR spectra, major functional groups in HPP

powder were identified, as presented in Fig. 4. The hydrophilicity of the HPP powder was indicated by the broad absorption band in the 3650–3000 cm^{-1} regions, attributable to the O–H groups presented in the components. The peak at 3288 cm^{-1} was attributed to intramolecular hydrogen bonding in cellulose II [52]. Furthermore, the peak at 2937 cm^{-1} was caused by cellulose aliphatic saturated C–H stretching vibration [53].

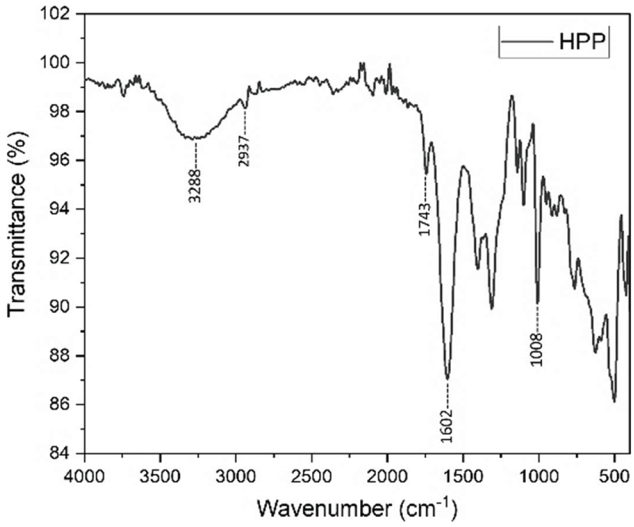

Figure 4: FTIR spectra of *Hylocereus Polyrhizus* peel powder

The presence of a peak located at ~1743 cm^{-1} indicated the presence of C=O stretching of the acetyl and uronic ester groups of polysaccharides, such as pectin, lignin, and hemicellulose [54,55]. The finding was almost similar to that reported by Ribeiro et al. [56] in untreated mandarin peels, where the peak was located around ~1750 cm^{-1}. The p-coumeric acids of lignin and/or hemicellulosic acids were also linked to this peak [57]. Peak 1602 cm^{-1} appeared to represent the stretching vibration of carboxyl ions (COO–) which indicated the presence of pectin in HPP powder [10]. This is according to the spectral region between 1500 and 1800 related to carboxylic acids and carboxylic esters, which are the key functional group responsible for the characteristics of pectin [58]. Furthermore, the carbohydrate fingerprint area found at wavenumber 800–1300 cm^{-1} can be utilized to identify the major chemical groups of polysaccharides [59].

3.5 X-ray Diffraction (XRD) Analysis

Hemicellulose and lignin are amorphous, whereas cellulose has both crystalline and amorphous domains in its structure [60]. The crystalline structure of cellulose influences its mechanical and thermal properties. The reinforcing ability and mechanical strength of cellulose, in particular, are critical characteristics for its use in environmental remediation technologies. Fig. 5 displays the X-ray diffractogram of the *Hylocereus Polyrhizus* peel powder. From the observation, there were three obvious peaks shown in the XRD pattern of the sample at diffraction angles of 14.55°, 22.17°, and 32.36°. The crystallinity pattern of cellulose for HPP powder was seen by the peak at $2\theta = 22.17°$ [61], which corresponded to the 200 lattice plane of cellulose I structure. Meanwhile, the characteristic peak of HPP powder identified at $2\theta = 14.55°$ and 32.36° were 110 and 004 lattice planes of cellulose I, indicating the presence of an amorphous region. Similar results were reported by Abiaziem et al. [44] for cellulose nanocrystal obtained from sugarcane peel and Huang et al. [62] for corncob pretreatment on the delignification and enzymatic hydrolysis.

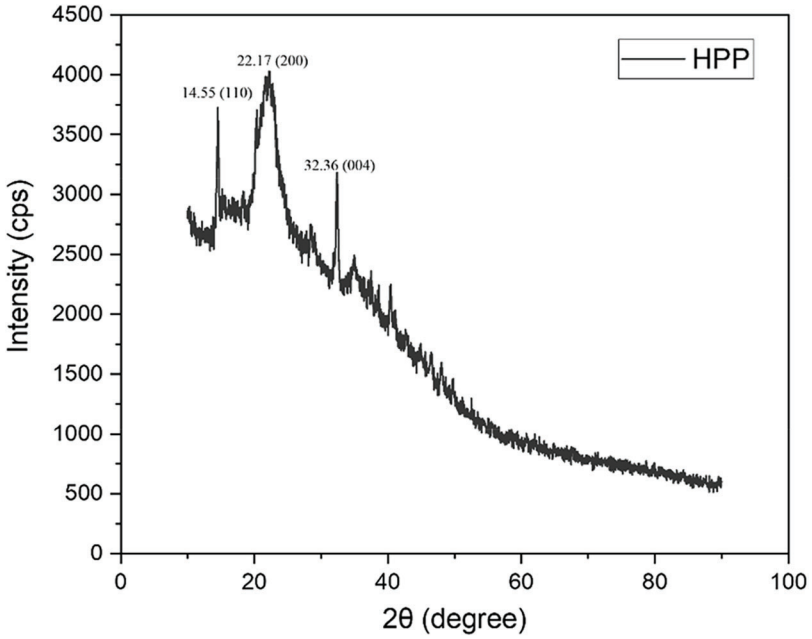

Figure 5: XRD pattern of *Hylocereus Polyrhizus* peel powder

Moreover, the crystallinity index for HPP powder was calculated using Eq. (1). which is described in the experimental section and found to be 32.76%. This result showed a high degree of crystallinity than cellulose from banana peels (15%) [53] and cellulose from *Pomelo albedo* (25.1%) [63], but lower than *Cucumis sativus* peels (56.7%) [35] and cassava root peel (56.3%) [64]. As a result, the crystallinity value varied based on the plant type and the method of fiber processing. The value of the crystallinity degree region and the material properties were related, with an increase in the crystallinity degree region enhancing the material's strength [46].

3.6 Thermogravimetric Analysis (TGA)

Thermal stability and weight loss of HPP powder were determined using thermogravimetric analysis (TGA) and differential thermogravimetric analysis (DTG). The TGA and DTG curves in Fig. 6 depict three distinct stages of weight loss (Table 4), as shown by significant peaks on the DTG curve. Overall, the weight loss of HPP powder occurred in the temperature range of 30°C–600°C. The initial weight loss was noticed in the TGA curve between 42°C and 108°C. The elimination of moisture and volatile organic compounds such as oils, terpenes, and pigments was responsible for this weight reduction [35,65,66]. The second weight loss was recorded between 204°C and 306°C, corresponding to the decomposition of cellulose [67]. The decomposition in the region of 318°C and 480°C referred to cellulose degradation; meanwhile, the lignin degradation took a wide temperature range between 100°C and 900°C [53,68].

In the DTG curves for HPP powder, three main peaks were observed located at 78°C (peak 1), 294°C (peak 2), and 479°C (peak 3), with mass losses of 7.16%, 34.92%, and 14.05%, respectively. The HPP powder demonstrated thermal decompositions of cellulose contents, as indicated by the strong U-shaped peak detected at 294°C. The presence of a final large thermal degradation peak near 479°C verified the degradation of the fiber's cellulose content as well as the removal of other non-cellulosic chemical elements. Overall, the thermal stability of the HPP powder was approximated to be 204°C, comparable to the thermal stability of *Dioscorea hispida* tubers [2].

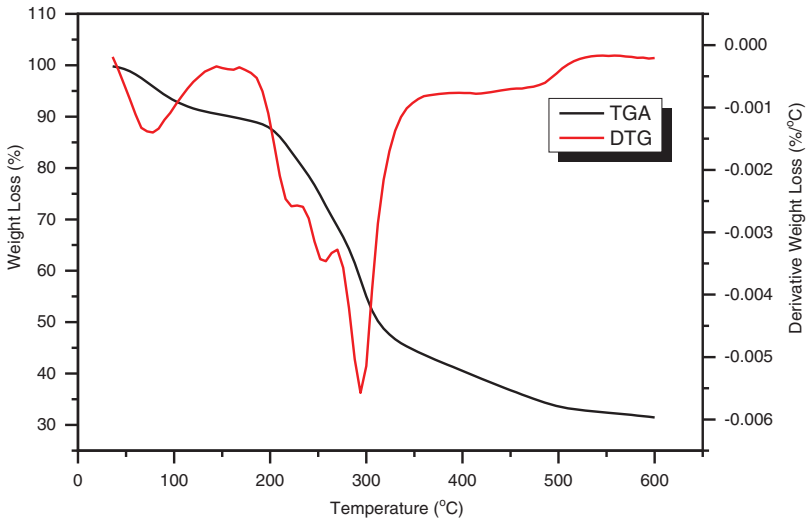

Figure 6: TGA and DTG curves of *Hylocereus Polyrhizus* peel powder

Table 4: Onset temperature (T_{onset}), thermal degradation on the maximum weight loss rate (T_{max}), weight loss (W_L), and char yield of *Hylocereus Polyrhizus* peel powder

Sample	Water evaporation			1st thermal degradation			2nd thermal degradation			Char yield
	T_{onset} (°C)	T_{max} (°C)	W_L (%)	T_{onset} (°C)	T_{max} (°C)	W_L (%)	T_{onset} (°C)	T_{max} (°C)	W_L (%)	W (%)
HPP	42	108	7.16	204	306	34.92	318	480	14.05	31.46

The residual char in the TGA analysis indicates the leftover or remaining materials after all volatile components were eliminated during the pyrolysis process [34]. Residual char of HPP powder was found to be 31.46%. This finding was parallel with the reported study conducted by Sahari et al. [69] that revealed the residues might be associated with the presence of inorganic material and silicon dioxide in the natural fiber, which can only be decomposed at a very high temperature. On the other hand, the composition of lignin and ash in *Hylocereus Polyrhizus* peel powder also contributed to char residue content.

4 Conclusions

The peel powder of *Hylocereus Polyrhizus* was successfully produced from *Hylocereus Polyrhizus* peel waste. The physical, chemical, morphological, and thermal characteristics of the *Hylocereus Polyrhizus* peel powder were all evaluated. The physical investigation of the HPP powder demonstrated that it had a large particle size suitable for a high-density application, low moisture content (9.70%), and higher water holding capacity (98.60%) if compared to cassava, corn stalk, and arrowroot fiber. Meanwhile, the chemical composition analyses showed that HPP powder has higher cellulose content (34.45%) than passion fruit peel fiber and prickly pear fruit peel. However, HPP powder showed lower lignin content (6.73%) compared to passion fruit peel. No trace of hemicellulose was detected in the HPP powder. The morphological study by SEM revealed that the peel surface appeared shriveled and had irregular geometry which was attributed to the high temperature during the drying process as well as the physical grinding process. FT-IR analysis showed the HPP powder contained pectin, a form of polysaccharides that offers an added value when combined with different types of biopolymers. The crystallinity index of HPP powder was 32.76%, which was higher than banana peels (15%) and cellulose from Pomelo albedo (25.1%). Thermal analysis revealed that HPP powder has a decomposition temperature of 204°C. This study revealed that the new approach to the development of sustainable bioproducts based on HPP powder has the potential to replace certain non-biodegradable and non-renewable polymer-based products in the market.

Acknowledgement: The authors would like to thank the Universiti Teknikal Malaysia Melaka for providing financial support under Grant No. RACER/2019/FTKMP-CARE/F00413 and Universiti Malaysia Sabah for financing the article processing charge for this study.

Funding Statement: This study was sponsored by the Universiti Teknikal Malaysia Melaka under Grant No. RACER/2019/FTKMP-CARE/F00413, as well as Universiti Malaysia Sabah for supported the article processing charge for this study.

Conflicts of Interest: The authors declare that they have no conflicts of interest to report regarding the present study.

References

1. Vinod, A., Sanjay, M. R., Suchart, S., Jyotishkumar, P. (2020). Renewable and sustainable biobased materials: An assessment on biofibers, biofilms, biopolymers and biocomposites. *Journal of Cleaner Production, 258,* 1–27. DOI 10.1016/j.jclepro.2020.120978.
2. Hazrati, K. Z., Sapuan, S. M., Zuhri, M. Y. M., Jumaidin, R. (2021). Extraction and characterization of potential biodegradable materials based on *Dioscorea hispida* tubers. *Polymers, 13(4),* 584. DOI 10.3390/polym13040584.
3. Mancini, E., Antonelli, M. G., Beomonte, P., Sasso, M. (2019). Characterization and analytical parametrization of composite in cellulose fibre and PVA matrix. *Composites Part B: Engineering, 172,* 496–505. DOI 10.1016/j.compositesb.2019.05.093.
4. Ibrahim, M. I. J., Sapuan, S. M., Zainudin, E. S., Zuhri, M. Y. M. (2019). Potential of using multiscale corn husk fiber as reinforcing filler in cornstarch-based biocomposites. *International Journal of Biological Macromolecules, 139,* 596–604. DOI 10.1016/j.ijbiomac.2019.08.015.
5. Hazrati, K. Z., Sapuan, S. M., Zuhri, M. Y. M., Jumaidin, R. (2021). Effect of plasticizers on physical, thermal, and tensile properties of thermoplastic films based on dioscorea hispida starch. *International Journal of Biological Macromolecules, 185,* 219–228. DOI 10.1016/j.ijbiomac.2021.06.099.
6. Pereira, P. H. F., de Freitas Rosa, M., Cioffi, M. O. H., de Carvalho Benini, K. C. C., Milanese, A. C. et al. (2015). Vegetal fibers in polymeric composites: A review. *Polimeros-Ciencia E Tecnologia, 25(1),* 9–22. DOI 10.1590/0104-1428.1722.
7. Tarique, J., Sapuan, S. M., Khalina, A. (2021). Extraction and characterization of a novel natural lignocellulosic (Bagasse and Husk) fibers from arrowroot (*Maranta Arundinacea*). *Journal of Natural Fibers, 11(3),* 1–17. DOI 10.1080/15440478.2021.1993418.
8. Ismail, N. S. M., Ramli, N., Hani, N. M., Meon, Z. (2012). Extraction and characterization of pectin from dragon fruit (*Hylocereus polyrhizus*) using various extraction conditions. *Sains Malaysiana, 41(1),* 41–45.
9. Hoe, K. (2017). Planting density of red pitaya (*Hylocereus Polyrhizus*) to achieve optimum yield under Malaysia weather condition. *International Journal of Agriculture Innovations and Research, 6(2),* 1473–2319.
10. Muhammad, N. W. F., Nurrulhidayah, A. F., Hamzah, M. S., Rashidi, O., Rohman, A. (2020). Physicochemical properties of dragon fruit peel pectin and citrus peel pectin: A comparison. *Food Research, 4(1),* 266–273. DOI 10.26656/fr.2017.4(S1).S14.
11. Listyarini, R. V., Susilawatib, P. R., Nukung, E. N., Anastasia, M., Yua, T. (2020). Bioplastic from pectin of dragon fruit (*Hylocereus polyrhizus*) peel. *Journal of Scientific and Applied Chemistry, 23(6),* 203–208. DOI 10.14710/jksa.23.6.203-208.
12. Rebecca, O. P. S., Harivaindaran, K. V., Boyce, A. N., Chandran, S. (2010). Potential natural dye with antioxidant properties from red dragon fruit (*Hylocereus polyrhizus*). *Acta Horticulturae, 875,* 477–486. DOI 10.17660/ActaHortic.2010.875.62.
13. Afandi, A., Lazim, A. M., Azwanida, N. N., Bakar, M. A., Airianah, O. B. et al. (2017). Antibacterial properties of crude aqueous *Hylocereus Polyrhizus* peel extracts in lipstick formulation against gram-positive and negative bacteria. *Malaysian Applied Biology, 46(2),* 29–34.

14. Mallampati, R., Xuanjun, L., Adin, A., Valiyaveettil, S. (2015). Fruit peels as efficient renewable adsorbents for removal of dissolved heavy metals and dyes from water. *ACS Sustainable Chemistry and Engineering, 3(6),* 1117–1124. DOI 10.1021/acssuschemeng.5b00207.
15. Mahlil, Y., Husmaini, W. M., Mahata, M. E. (2018). Using physical and chemical methods to improve the nutrient quality of dragon fruit (*Hylocereus polyrhizus*) peel for use as feed for laying hens. *International Journal of Poultry Science, 17(2),* 51–56. DOI 10.3923/ijps.2018.51.56.
16. Lee, T. W., Tsai, I. C., Liu, Y. F., Chen, C. (2022). Upcycling fruit peel waste into a green reductant to reduce graphene oxide for fabricating an electrochemical sensing platform for sulfamethoxazole determination in aquatic environments. *Science of the Total Environment, 812,* 152273. DOI 10.1016/j.scitotenv.2021.152273.
17. Fatiha, L., Dwyana, Z., Johannes, E. (2022). Silver nanoparticles synthesis from dragon fruit (*Hylocereus polyrhizus*) peel extract and its potential as antiseptic mouthwash. *Proceedings of the 2nd International Conference on Education and Technology (ICETECH 2021),* vol. 630, pp. 380–386. DOI 10.2991/assehr.k.220103.054.
18. Prastiya, R. A., Yusuf, A. M. (2021). Red dragon fruit peel (*Hylocereus polyrhizus*) as feed biosupplement on performance of fattening rabbits. *IOP Conference Series: Earth and Environmental Science, 743(1),* 3–8. DOI 10.1088/1755-1315/743/1/012060.
19. Bakar, J., Shu, C. E., Kharidah, M., Dzulkifly, M. A., Noranizan, A. (2011). Physico-chemical characteristics of red pitaya (*Hylocereus Polyrhizus*) peel. *International Food Research Journal, 18(1),* 279–286.
20. Mastersizer 3000 user manual. (2013). https://www.malvernpanalytical.com/en/.
21. Szecsődi, O., Makó, A., Labancz, V., Barna, G., Gálos, B. et al. (2021). Using different approaches of particle size analysis for estimation of water retention capacity of soils: Example of keszthely mountains (Hungary). *Acta Silvatica et Lignaria Hungarica, 17(1),* 37–50. DOI 10.37045/aslh-2021-0003.
22. Ibrahim, M. I. J., Sapuan, S. M., Zainudin, E. S., Zuhri, M. Y. M. (2019). Extraction, chemical composition, and characterization of potential lignocellulosic biomasses and polymers from corn plant parts. *BioResources, 14(3),* 6485–6500. DOI 10.15376/biores.14.3.6485-6500.
23. Segal, L., Creely, J. J., Martin, A. E., Conrad, C. M. (1959). An empirical method for estimating the degree of crystallinity of native cellulose using the X-ray diffractometer. *Textile Research Journal, 29(10),* 786–794. DOI 10.1177/004051755902901003.
24. Fu, S. Y., Feng, X. Q., Lauke, B., Mai, Y. W. (2008). Effects of particle size, particle/matrix interface adhesion and particle loading on mechanical properties of particulate-polymer composites. *Composites Part B: Engineering, 39(6),* 933–961. DOI 10.1016/j.compositesb.2008.01.002.
25. Campbell, F. C. (2010). *Structural composite materials*. Materials Park, Ohio: ASM International.
26. Edhirej, A., Sapuan, S. M., Jawaid, M., Zahari, N. I. (2015). Cassava: Its polymer, fiber, composite, and application. *Polymer Composites, 38(3),* 555–570.
27. Tarique, J., Sapuan, S. M., Khalina, A., Sherwani, S. F. K., Yusuf, J. et al. (2021). Recent developments in sustainable arrowroot (*Maranta arundinacea* Linn) starch biopolymers, fibres, biopolymer composites and their potential industrial applications: A review. *Journal of Materials Research and Technology, 13,* 1191–1219. DOI 10.1016/j.jmrt.2021.05.047.
28. Deepthi, P. V., Raju, K. S. R., Reddy, M. I. (2019). Dynamic mechanical analysis of banana, pineapple leaf and glass fibre reinforced hybrid polyester composites. *Materials Today: Proceedings, 18,* 2114–2117. DOI 10.1016/j.matpr.2019.06.484.
29. Chia, S. L., Chong, G. H. (2015). Effect of drum drying on physico-chemical characteristics of dragon fruit peel (*Hylocereus polyrhizus*). *International Journal of Food Engineering, 11(2),* 285–293. DOI 10.1515/ijfe-2014-0198.
30. Bakar, J., Ee, S. C., Muhammad, K., Hashim, D. M., Adzahan, N. (2013). Spray-drying optimization for red pitaya peel (*Hylocereus polyrhizus*). *Food and Bioprocess Technology, 6(5),* 1332–1342. DOI 10.1007/s11947-012-0842-5.
31. Ee, S. C., Bakar, J., Kharidah, M., Dzulkifly, M. H., Noranizan, A. (2014). Physico-chemical properties of spray-dried red pitaya (*Hylocereus polyrhizus*) peel powder during storage. *International Food Research Journal, 21(3),* 1177–1182.
32. Yusriah, L., Sapuan, S. M., Zainudin, E. S., Mariatti, M. (2014). Characterization of physical, mechanical, thermal and morphological properties of agro-waste betel nut (*Areca catechu*) husk fibre. *Journal of Cleaner Production, 72,* 174–180. DOI 10.1016/j.jclepro.2014.02.025.

33. Edhirej, A., Sapuan, S. M., Jawaid, M., Zahari, N. I. (2016). Preparation and characterization of cassava starch/peel composite film. *Polymer Composites, 39(5),* 1704–1715. DOI 10.1002/pc.
34. Razali, N., Salit, M. S., Jawaid, M., Ishak, M. R., Lazim, Y. (2015). A study on chemical composition, physical, tensile, morphological, and thermal properties of roselle fibre: Effect of fibre maturity. *BioResources, 10(1),* 1803–1823. DOI 10.15376/biores.10.1.1803-1824.
35. Sai Prasanna, N., Mitra, J. (2020). Isolation and characterization of cellulose nanocrystals from cucumis sativus peels. *Carbohydrate Polymers, 247,* 1–10. DOI 10.1016/j.carbpol.2020.116706.
36. Orozco, R. S., Hernández, P. B., Morales, G. R., Núñez, F. U., Villafuerte, J. O. et al. (2014). Characterization of lignocellulosic fruit waste as an alternative feedstock for bioethanol production. *BioResources, 9(2),* 1873–1885.
37. Chen, R. S., Salleh, M. N., Ab Ghani, M. H., Ahmad, S., Gan, S. (2015). Biocomposites based on rice husk flour and recycled polymer blend: Effects of interfacial modification and high fibre loading. *BioResources, 10(4),* 6872–6885. DOI 10.15376/biores.10.4.6872-6885.
38. Patil, A. Y., Hrishikesh, N. U., Basavaraj, G. D., Chalageri, G. R., Kodancha, K. G. (2018). Influence of biodegradable natural fiber embedded in polymer matrix. *Materials Today: Proceedings, 5(2),* 7532–7540. DOI 10.1016/j.matpr.2017.11.425.
39. Harussani, M. M., Sapuan, S. M., Khalina, A., Ilyas, R. A., Hazrol, M. D. (2020). Review on green technology pyrolysis for plastic wastes. *7th Postgraduate Seminar on Natural Fibre Reinforced Polymer Composites,* pp. 50–53.
40. Diyana, Z. N., Jumaidin, R., Selamat, M. Z., Alamjuri, R. H., Yusof, F. A. M. (2021). Extraction and characterization of natural cellulosic fiber from *Pandanus amaryllifolius* leaves. *Polymers, 13(23),* 1–16. DOI 10.3390/polym13234171.
41. Shamsuyeva, M., Endres, H. J. (2021). Plastics in the context of the circular economy and sustainable plastics recycling: Comprehensive review on research development, standardization and market. *Composites Part C: Open Access, 6,* 1–16. DOI 10.1016/j.jcomc.2021.100168.
42. Uitterhaegen, E., Parinet, J., Labonne, L., Mérian, T., Ballas, S. et al. (2018). Performance, durability and recycling of thermoplastic biocomposites reinforced with coriander straw. *Composites Part A: Applied Science and Manufacturing, 113,* 254–263. DOI 10.1016/j.compositesa.2018.07.038.
43. Habibi, Y., Mahrouz, M., Vignon, M. R. (2009). Microfibrillated cellulose from the peel of prickly pear fruits. *Food Chemistry, 115(2),* 423–429. DOI 10.1016/j.foodchem.2008.12.034.
44. Abiaziem, C. V., Williams, A. B., Inegbenebor, A. I., Onwordi, C. T., Ehi-Eromosele, C. O. et al. (2020). Isolation and characterisation of cellulose nanocrystal obtained from sugarcane peel. *Rasayan Journal of Chemistry, 13(1),* 177–187. DOI 10.31788/RJC.2020.1315328.
45. Wijaya, C. J., Saputra, S. N., Soetaredjo, F. E., Putro, J. N., Lin, C. X. et al. (2017). Cellulose nanocrystals from passion fruit peels waste as antibiotic drug carrier. *Carbohydrate Polymers, 175,* 370–376. DOI 10.1016/j.carbpol.2017.08.004.
46. Ilyas, R. A., Sapuan, S. M., Ishak, M. R. (2018). Isolation and characterization of nanocrystalline cellulose from sugar palm fibres (*Arenga Pinnata*). *Carbohydrate Polymers, 181,* 1038–1051. DOI 10.1016/j.carbpol.2017.11.045.
47. Kamaruddin, Z. H., Jumaidin, R., Rushdan, A. I., Selamat, M. Z., Alamjuri, R. H. (2021). Characterization of natural cellulosic fiber isolated from Malaysian *Cymbopogan citratus* leaves. *BioResources, 16(4),* 7729–7750. DOI 10.15376/biores.16.4.7729-7750.
48. Nagarajasetty, V. K. S., Goud, G., Rangappa, S. M., Siengchin, S. (2022). Limonia acidissima (wood-apple) shell: Micro and nanoparticles preparation and chemical treatment. *Materials Today: Proceedings, 52,* 2543–2547. DOI 10.1016/j.matpr.2021.12.049.
49. Tonon, R. V., Brabet, C., Hubinger, M. D. (2008). Influence of process conditions on the physicochemical properties of açai (*Euterpe oleraceae* Mart.) powder produced by spray drying. *Journal of Food Engineering, 88(3),* 411–418. DOI 10.1016/j.jfoodeng.2008.02.029.
50. Alamilla-Beltrán, L., Chanona-Pérez, J. J., Jiménez-Aparicio, A. R., Gutiérrez-Lopez, G. F. (2005). Description of morphological changes of particles along spray drying. *Journal of Food Engineering, 67(1–2),* 179–184. DOI 10.1016/j.jfoodeng.2004.05.063.

51. Gan, L., Guo, H., Xiao, Z., Jia, Z., Yang, H. et al. (2019). Dyeing and characterization of cellulose powder developed from waste cotton. *Polymers, 11(12),* 1982. DOI 10.3390/polym11121982.
52. Zuluaga, R., Putaux, J. L., Cruz, J., Vélez, J., Mondragon, I. et al. (2009). Cellulose microfibrils from banana rachis: Effect of alkaline treatments on structural and morphological features. *Carbohydrate Polymers, 76(1),* 51–59. DOI 10.1016/j.carbpol.2008.09.024.
53. Pelissari, F. M., Sobral, P. J. D. A., Menegalli, F. C. (2014). Isolation and characterization of cellulose nanofibers from banana peels. *Cellulose, 21(1),* 417–432. DOI 10.1007/s10570-013-0138-6.
54. Sain, M., Panthapulakkal, S. (2006). Bioprocess preparation of wheat straw fibers and their characterization. *Industrial Crops and Products, 23(1),* 1–8. DOI 10.1016/j.indcrop.2005.01.006.
55. Sgriccia, N., Hawley, M. C., Misra, M. (2008). Characterization of natural fiber surfaces and natural fiber composites. *Composites Part A: Applied Science and Manufacturing, 39(10),* 1632–1637. DOI 10.1016/j.compositesa.2008.07.007.
56. Ribeiro, G. C., Coelho, L. M., Oliveira, E., Coelho, N. M. M. (2013). Removal of Cu(II) from ethanol fuel using mandarin peel as biosorbent. *BioResources, 8(3),* 3309–3321. DOI 10.15376/biores.8.3.3309-3321.
57. Alemdar, A., Sain, M. (2008). Isolation and characterization of nanofibers from agricultural residues-wheat straw and soy hulls. *Bioresource Technology, 99(6),* 1664–1671. DOI 10.1016/j.biortech.2007.04.029.
58. Coelho, E. M., de Azevedo, L. C., Viana, A. C., Ingrid, G. R., Raquel, G. G. et al. (2017). Physico-chemical properties, rheology and degree of esterification of passion fruit (*Passiflora edulis* f. *Flavicarpa*) peel flour. *Journal of the Science of Food and Agriculture, 98(1),* 166–173. DOI 10.1002/jsfa.8451.
59. Zaidel, D. N. A., Rashid, J. M., Hamidon, N. H., Salleh, L. M., Kassim, A. S. M. (2017). Extraction and characterisation of pectin from dragon fruit (*Hylocereus Polyrhizus*) peels. *Chemical Engineering Transactions, 56,* 805–810. DOI 10.3303/CET1756135.
60. Liu, Y., Liu, A., Ibrahim, S. A., Yang, H., Huang, W. (2018). Isolation and characterization of microcrystalline cellulose from pomelo peel. *International Journal of Biological Macromolecules, 111,* 717–721. DOI 10.1016/j.ijbiomac.2018.01.098.
61. Sofla, M. R. K., Brown, R. J., Tsuzuki, T., Rainey, T. J. (2016). A comparison of cellulose nanocrystals and cellulose nanofibres extracted from bagasse using acid and ball milling methods. *Advances in Natural Sciences: Nanoscience and Nanotechnology, 7(3),* 35004. DOI 10.1088/2043-6262/7/3/035004.
62. Huang, Z., Liu, C., Feng, X., Wu, M., Tang, Y. et al. (2020). Effect of regeneration solvent on the characteristics of regenerated cellulose from lithium bromide trihydrate molten salt. *Cellulose, 27(16),* 9243–9256. DOI 10.1007/s10570-020-03440-y.
63. Zain, N. F. M., Yusop, S. M., Ahmad, I. (2014). Preparation and characterization of cellulose and nanocellulose from pomelo (*Citrus grandis*) albedo. *Journal of Nutrition & Food Sciences, 5(1),* 10–13. DOI 10.4172/2155-9600.1000334.
64. Leite, A. L. M. P., Zanon, C. D., Menegalli, F. C. (2017). Isolation and characterization of cellulose nanofibers from cassava root bagasse and peelings. *Carbohydrate Polymers, 157,* 962–970. DOI 10.1016/j.carbpol.2016.10.048.
65. Dai, H., Ou, S., Huang, Y., Huang, H. (2018). Utilization of pineapple peel for production of nanocellulose and film application. *Cellulose, 25(3),* 1743–1756. DOI 10.1007/s10570-018-1671-0.
66. Pathak, P. D., Mandavgane, S. A., Kulkarni, B. D. (2017). Fruit peel waste: Characterization and its potential uses. *Current Science, 113(3),* 444–454. DOI 10.18520/cs/v113/i03/444-454.
67. Deepa, B., Abraham, E., Cherian, B. M., Bismarck, A., Blaker, J. J. et al. (2011). Structure, morphology and thermal characteristics of banana nano fibers obtained by steam explosion. *Bioresource Technology, 102(2),* 1988–1997. DOI 10.1016/j.biortech.2010.09.030.
68. Yang, H., Yan, R., Chen, H., Lee, D. H., Zheng, C. (2007). Characteristics of hemicellulose, cellulose and lignin pyrolysis. *Fuel, 86(12–13),* 1781–1788. DOI 10.1016/j.fuel.2006.12.013.
69. Sahari, J., Sapuan, S. M., Zainudin, E. S., Maleque, M. A. (2013). Mechanical and thermal properties of environmentally friendly composites derived from sugar palm tree. *Materials and Design, 49,* 285–289. DOI 10.1016/j.matdes.2013.01.